Available online at www.sciencedirect.com
SCIENCE DIRECT
ELSEVIER
Journal of the European Ceramic Society 26 (2006) 2063–2068
ECERS
www.elsevier.com/locate/jeurceramsoc

Low temperature sintering and microwave dielectric properties of $(Mg_{3-x}Zn_x)(VO_4)_2$ ceramics

Ryosuke Umemura *, Hirotaka Ogawa, Akinori Kan

Faculty of Science and Technology, Meijo University, 1-501 Shiogamaguchi, Tenpaku-ku, Nagoya 468-8502, Japan

Available online 21 November 2005

Abstract

This paper describes the effects of Zn substitution for Mg on the microwave dielectric properties of $(Mg_{3-x}Zn_x)(VO_4)_2$ ceramics. As for the XRPD patterns of $(Mg_{3-x}Zn_x)(VO_4)_2$ ceramics sintered at the sintering temperature of 750 °C, no secondary phase was detected over the whole composition range. However, in the case of the sample sintered at 850 °C, the $Zn_4V_2O_9$ and $Zn_2V_2O_7$ compounds were identified by using XRPD; this result was attributed to the decomposition of $Zn_3(VO_4)_2$ phase. From crystal structure analysis, it was found that the atomic distances of $M(1)$—O (M = Mg and Zn) and $M(2)$—O in MO_6 octahedra increased, though that of V—O in VO_4 tetrahedron decreased. Moreover, the slight tilting of $M(2)O_6$ octahedron was observed by the Zn substitution. As for the covalency of cation–oxygen bond, the covalency of M—O bond in $M(1)O_6$ and $M(2)O_6$ octahedra decreased because of the increase in the atomic distance of M—O, whereas that of V—O increased with increasing the Zn addition. However, as a result, the slight decrease in the covalency of cation–oxygen bond was recognized because the variation in the covalency of M—O bond is predominant in this crystal structure. The dielectric constants of the samples range from 4.4 to 11.1. The decrease in the covalency may be related to the difference in the dielectric constant of each composition. The maximum $Q \cdot f$ value of bulk densities is effected by varying the chemical composition of $(Mg_{3-x}Zn_x)(VO_4)_2$ ceramics and it shifts toward lower sintering temperature with an increase in x within the temperature region of 800–1050 °C. The temperature coefficient of resonant frequency (τ_f) of the samples decreased with increasing of Zn, and then a variation in τ_f value was attributed to the tilting of $M(2)O_6$ octahedron caused by Zn substitution for Mg.

Keywords: Powders-solid state reaction; Grain growth; ZnO; X-ray method

1. Introduction

In recent years, an increasing effort has been directed toward attaining the miniaturization of components with the multilayer microwave integrated devices, i.e., integrations of passive components such as inductors, resistors, capacitors and line resonators into the substrate which carries the integrated circuits. However, in order to make the multilayer microwave integrated devices, the development of low temperature co-fired ceramics (LTCC) is required. The sintering temperature for LTCC has to be lower than 960.5 °C, which is the melting point of Ag which is used as an electrode material. For the commercial application such as a resonation at microwave frequency, a requirement of a high $Q \cdot f$, a high permittivity and a stable temperature coefficient of resonant frequency (τ_f) is necessary. For LTCC material, which are widely used as a substrate for the application to the multilayered microwave devices, a low dielectric constant with high $Q \cdot f$ is required. Thus, there is considerable interest in a development of a new LTCC material with high $Q \cdot f$.

In MgO–V_2O_5 system, Kerby and Wilson[1] reported that the $Mg_3(VO_4)_2$ compound was partially melted at 980 °C. Therefore, the $Mg_3(VO_4)_2$ compound was considered to be an appropriate candidate for new LTCC material. The microwave dielectric properties of $Mg_3(VO_4)_2$ compound sintered at 1050 °C for 5 h were reported to have a dielectric constant (ε_r) of 9.3 and a quality factor($Q \cdot f$) of 65440 GHz with a temperature coefficient of resonant frequency (τ_f) of −89.5 ppm/°C.[2] However, the sintering temperature of $Mg_3(VO_4)_2$ is still too high to use together with an internal conductor such as a silver because the melting point of silver is 960.5 °C. In the case of the ZnO–V_2O_5 system, it was reported that the $Zn_3(VO_4)_2$ compound decomposed to form the $Zn_4V_2O_9$ and $Zn_2V_2O_7$ compounds at 815 °C, followed by a partial melting at 860 °C.[3] Thus, the Zn substitution for Mg may be effective in reducing the sintering temperature of a new $(Mg_{3-x}Zn_x)(VO_4)_2$ ceramic. The effects of Zn substitution for Mg on the crystal structure, microstructure, reduction of sintering temperature

* Corresponding author.

0955-2219/$ – see front matter © 2005 Elsevier Ltd. All rights reserved.
doi:10.1016/j.jeurceramsoc.2005.09.099

and microwave dielectric properties of $(Mg_{3-x}Zn_x)(VO_4)_2$ were investigated in this paper.

2. Experimental method

The samples of $(Mg_{3-x}Zn_x)(VO_4)_2$ ceramics were prepared by a conventional solid state reaction method from individual reagent-grade oxide powders: MgO (99.9% purity), ZnO (99.9% purity) and V_2O_5 (99.99% purity). The powders were weighed according to the stoichiometric compositions of $(Mg_{3-x}Zn_x)(VO_4)_2$, and then mixed with a mortar for 45 min in ethanol. The obtained powers were calcined at the temperature of 700 °C for 20 h in air. The calcined powders were ground for 45 min in ethanol with a suitable amount of 5% solution of polyvinyl alcohol (PVA) as the binder and formed into pellets (12 mm in diameter and 7 mm thickness) via uniaxial pressing at 100 MPa in a stainless-steel die. These pellets were sintered in the temperatures range of 750–1075 °C for 5 h in air, using the heating and cooling rates of 5 °C/min. The crystalline phases of the samples were identified by X-ray powder diffraction (XRPD) using Cu Kα radiation, where the crystalline phases of the samples were refined by Rietveld analysis.[4,5] The microstructure observations of the sintered surfaces were performed by means of field emission scanning electron microscope (FE-SEM) and energy dispersive X-ray analysis (EDX). The bulk densities of the sintered samples were measured by Archimedes method. The temperature coefficient of dielectric constant (τ_ε) of the sample was measured at a frequency of 1 MHz using LCR meter. The microwave dielectric properties of the samples were evaluated in terms of the Hakki and Coleman method.[6]

3. Results and discussion

The crystal structure of $(Mg_{3-x}Zn_x)(VO_4)_2$ ceramics was investigated by using XRPD. Fig. 1 shows the XRPD patterns of $(Mg_{3-x}Zn_x)(VO_4)_2$ ceramics sintered at 750 °C for 5 h in air. No secondary phase was detected in the composition range of 0–3. In order to confirm the solid solutions, the lattice parameters of $(Mg_{3-x}Zn_x)(VO_4)_2$ ceramics sintered at 750 °C for 5 h in air were refined by using Rietveld analysis. The plot of refined lattice parameters versus composition x of $(Mg_{3-x}Zn_x)(VO_4)_2$ ceramics are shown in Fig. 2. The lattice parameters, a and b, linearly increased with increased x, whereas the lattice parameter c decreased. Fig. 3 shows the crystal structure of $Mg_3(VO_4)_2$ ceramic which has an orthorhombic structure with space group of *Cmca* (No. 64). The crystal structure of the ceramic is composed to the $M(1)O_6$ (where M = Mg and Zn) and $M(2)O_6$ octahedra, and VO_4 tetrahedron, where these polyhedra linked each other as shown in Fig. 3. The influence of Zn substitution for Mg on the atomic distances of cation–oxygen bonds is shown in Table 1 where an increase in the atomic distance of M–O is observed with increasing Zn and the atomic distance of V–O was decreased. Moreover, with increased x, a slight tilting of $M(2)O_6$ octahedron was recognized as shown in Fig. 4. Thus, it is considered that the increase in the lattice parameters a and b are due to the increase in the atomic distances of M–O bond in MO_6 octahedron. Moreover, the decrease in the lattice parame-

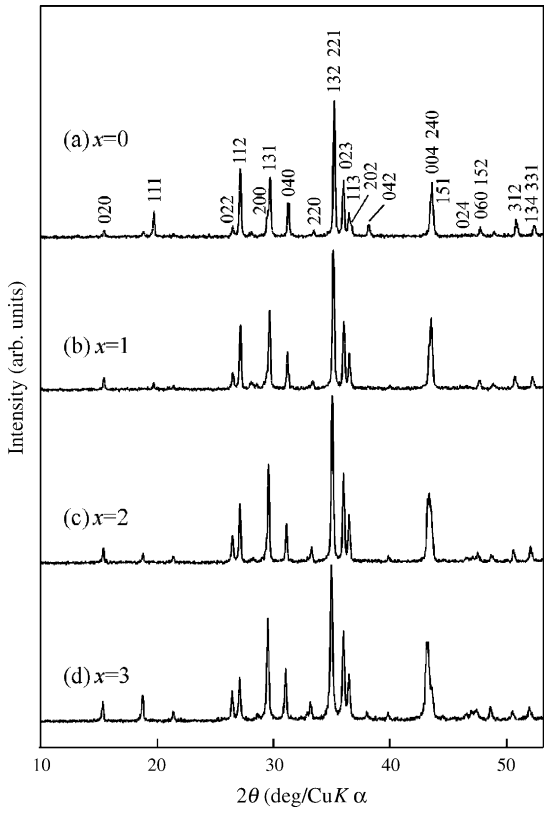

Fig. 1. XRPD patterns of the $(Mg_{3-x}Zn_x)(VO_4)_2$ ceramics sintered at 750 °C for 5 h in air.

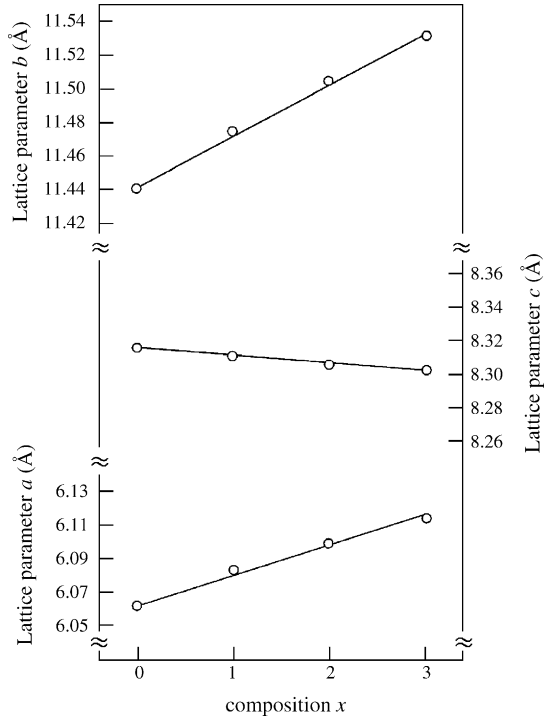

Fig. 2. Lattice parameters of $(Mg_{3-x}Zn_x)(VO_4)_2$ ceramics sintered at 750 °C for 5 h in air as a function of composition x.

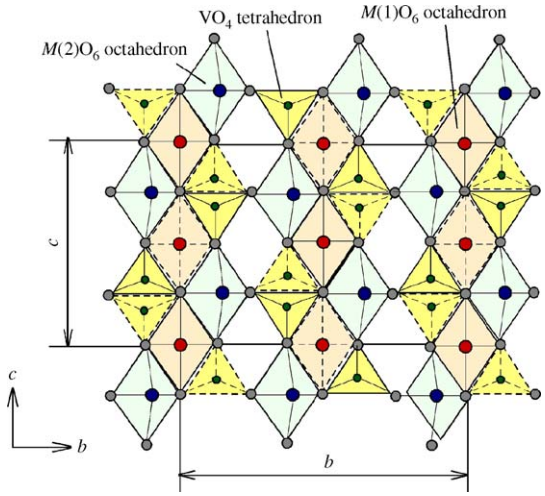

Fig. 3. Crystal structure of $Mg_3(VO_4)_2$ ceramic.

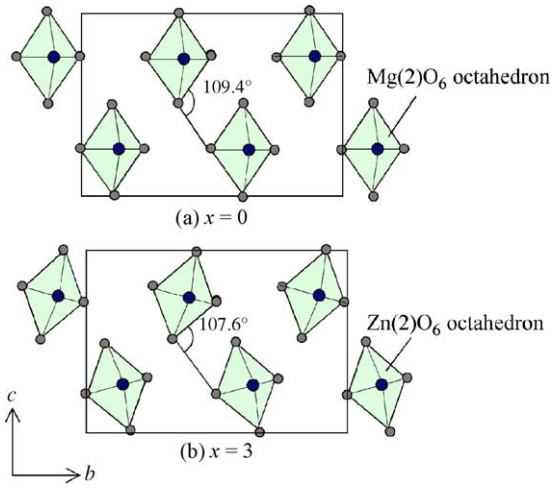

Fig. 4. Tilting of $M(2)O_6$ octahedron (M = Mg and Zn) caused by Zn substitution for Mg.

ter c is attributed to the tilting of $M(2)O_6$ octahedron. As for the covalency of cation–oxygen bond, the cation–oxygen bond in the polyhedra was determined on the basis of the bond valance theorem.[7] The normalized covalency of each cation–oxygen bond is shown in Fig. 5, where the normalized covalency of M–O bond decreased, whereas that of V–O bond increased with increased x. These variations in the normalized covalency are closely related to those of atomic distances caused by the Zn substitution for Mg. As a result, the covalency of cation–oxygen bond seems to decrease by the Zn substitution for Mg because the variations in covalency of $M(1)$–O and $M(2)$–O bonds are higher in comparison with that of V–O bond.

Table 1
Atomic distances and volumes of $M(1)O_6$, $M(2)O_6$ (M = Mg and Zn) and VO_4 polyhedra

Composition	Atomic distance (Å)		Polyhedron volume (Å^3)	
$x=0$	$M(1)$—O(2) × 2	2.040 (5)	$M(1)O_6$	12.4371
	$M(1)$—O(3) × 2	2.151 (4)		
	$M(2)$—O(1) × 2	2.002 (5)		
	$M(2)$—O(2) × 2	2.141 (6)	$M(2)O_6$	11.9392
	$M(2)$—O(3) × 2	2.104 (4)		
	V—O(1)	1.750 (7)		
	V—O(2)	1.813 (7)	VO_4	2.7277
	V—O(3) × 2	1.712 (4)		
$x=1$	$M(1)$—O(2) × 2	2.036 (7)	$M(1)O_6$	12.5544
	$M(1)$—O(3) × 2	2.166 (4)		
	$M(2)$—O(1) × 2	2.018 (5)		
	$M(2)$—O(2) × 2	2.163 (6)	$M(2)O_6$	12.2142
	$M(2)$—O(3) × 2	2.112 (4)		
	V—O(1)	1.729 (7)		
	V—O(2)	1.804 (8)	VO_4	2.6642
	V—O(3) × 2	1.699 (4)		
$x=2$	$M(1)$—O(2) × 2	2.026 (9)	$M(1)O_6$	12.6714
	$M(1)$—O(3) × 2	2.182 (5)		
	$M(2)$—O(1) × 2	2.044 (6)		
	$M(2)$—O(2) × 2	2.199 (7)	$M(2)O_6$	12.7886
	$M(2)$—O(3) × 2	2.144 (5)		
	V—O(1)	1.694 (9)		
	V—O(2)	1.770 (10)	VO_4	2.5660
	V—O(3) × 2	1.691 (6)		
$x=3$	$M(1)$—O(2) × 2	2.038 (9)	$M(1)O_6$	13.1775
	$M(1)$—O(3) × 2	2.222 (5)		
	$M(2)$—O(1) × 2	2.038 (6)		
	$M(2)$—O(2) × 2	2.247 (7)	$M(2)O_6$	13.1287
	$M(2)$—O(3) × 2	2.158 (5)		
	V—O(1)	1.709 (9)		
	V—O(2)	1.712 (10)	VO_4	2.4558
	V—O(3) × 2	1.658 (5)		

Variations of bulk density and dielectric constant (ε_r) as a function of sintering temperature are shown in Figs. 6 and 7, respectively. The ε_r values of well-sintered $(Mg_{3-x}Zn_x)(VO_4)_2$ ceramics range from 9 to 11. These values are similar to that of low-temperature sintered Al_2O_3[8] which is suitable as a substrate for the multilayer microwave integrated circuit device. It is shown in the bulk density and ε_r curves that these saturated values depend on the chemical composition and shift toward low sintering temperatures with increasing the composition x. This result is attributed to the partial melting of $(Mg_{3-x}Zn_x)(VO_4)_2$ ceramics and therefore it was found that the Zn substitution for Mg was effective in reducing the sintering temperature from

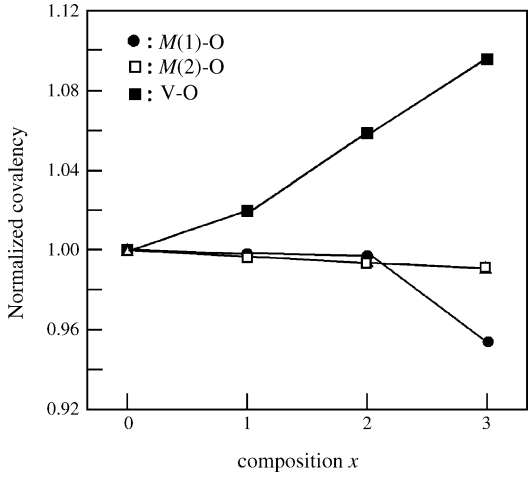

Fig. 5. Normalized covalency of cation–oxygen bond in $M(1)O_6$, $M(2)O_6$ (M = Mg and Zn) and VO_4 polyhedra with increasing x.

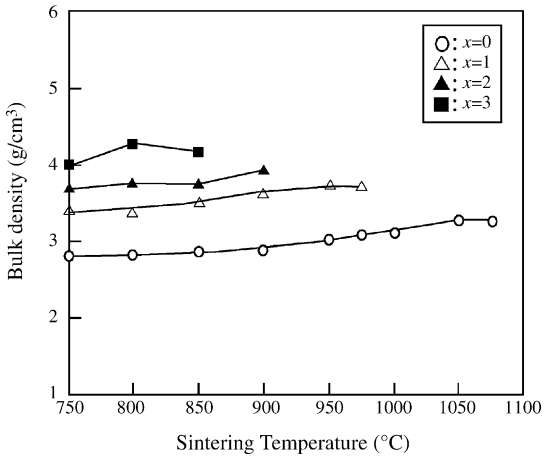

Fig. 6. Sintering temperature dependence of the bulk density of $(Mg_{3-x}Zn_x)(VO_4)_2$ ceramics.

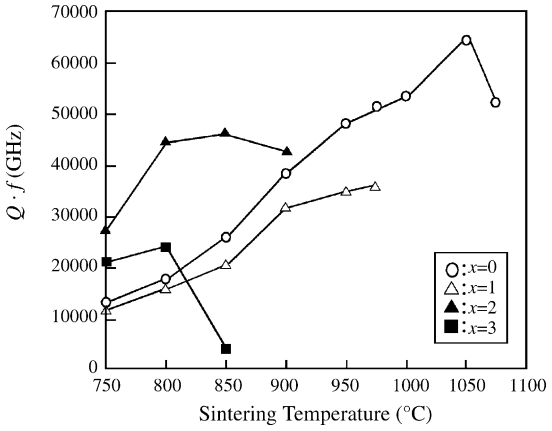

Fig. 8. Relationship between the $Q \cdot f$ values and sintering temperature of $(Mg_{3-x}Zn_x)(VO_4)_2$ ceramics.

1050 to 800 °C. When comparing the dielectric constant of the samples at $x = 0$ with those at $x = 1$, 2 and 3 sintered at the same temperature, the dielectric constant of the samples increased with increased amount of Zn. This was explained by the decrease of the covalency of *M*–O bond.

The relationships between $Q \cdot f$ and sintering temperature in the $(Mg_{3-x}Zn_x)(VO_4)_2$ ceramics are shown in Fig. 8. In general, the $Q \cdot f$ values of $(Mg_{3-x}Zn_x)(VO_4)_2$ ceramics increased with increasing sintering temperatures; however, the $Q \cdot f$ value of undoped $Mg_3(VO_4)_2$ sintered at 1075 °C had lower $Q \cdot f$ than the sample sintered at 1050 °C. The decrease of $Q \cdot f$ is due to the decomposition of $Mg_3(VO_4)_2$ into a liquid phase which takes place at 1074 °C. In the case of $x = 3$, the $Q \cdot f$ value of $Zn_3(VO_4)_2$ compound decreased above 800 °C. The decrease in the $Q \cdot f$ value may relate to the decomposition of the $Zn_3(VO_4)_2$. Fig. 9 shows the XRPD patterns of $Zn_3(VO_4)_2$ compound sintered at 750, 800 and 850 °C for 5 h in air. The two phases, i.e., $Zn_4V_2O_9$ and $Zn_2V_2O_7$, were only detected in the XRPD patterns when the sintering temperature was 850 °C and hence, a single phase of $Zn_3(VO_4)_2$ was obtained at the sintering temperature below 850 °C as shown in Fig. 9(a) and (b). The decomposition of the $Zn_3(VO_4)_2$ into $Zn_4V_2O_9$ and $Zn_2V_2O_7$ was consistent with the binary phase diagram of the ZnO–V_2O_5 system reported by Makarov et al.[3]

In order to clarify the relationship microwave dielectric properties and the morphological changes in the sample, the microstructure of the $(Mg_{3-x}Zn_x)(VO_4)_2$ compounds sintered at 850 °C for 5 h in air was investigated in terms of FE-SEM as shown in Fig. 10. The changes in the grain size can be seen in the composition ranging from 0 to 2. The variation of the $Q \cdot f$ between different amounts of Zn in the $(Mg_{3-x}Zn_x)(VO_4)_2$ compounds is attributed to the morphological changes in the samples. It is found that the Zn substitution for Mg enhances the grain growth at low sintering temperature and the grain growth plays an important role in the $Q \cdot f$ value of $(Mg_{3-x}Zn_x)(VO_4)_2$ ceramics. However, a non-homogeneous grain growth at $x = 3$

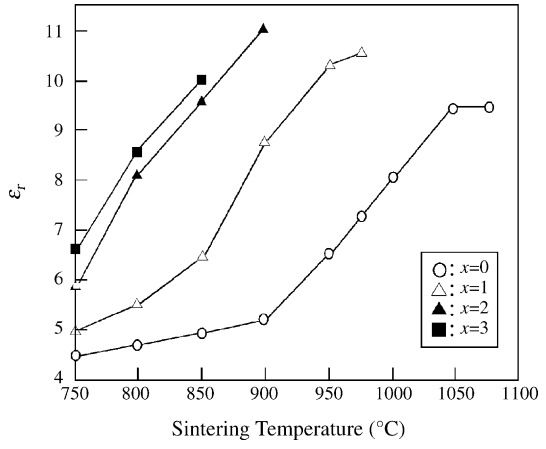

Fig. 7. Variations of the dielectric constant of $(Mg_{3-x}Zn_x)(VO_4)_2$ ceramics sintered for 5 h in air as a function of sintering temperature.

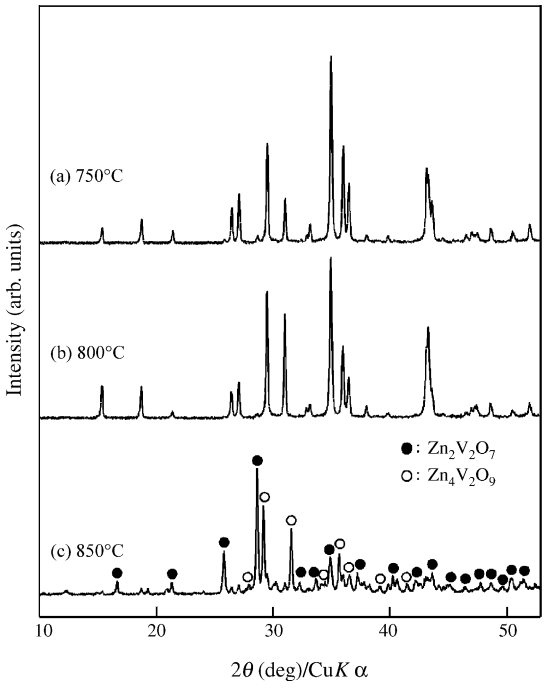

Fig. 9. XRPD patterns of $Zn_3(VO_4)_2$ ceramic sintered at: (a) 750°C, (b) 800°C and (c) 850 °C for 5 h in air.

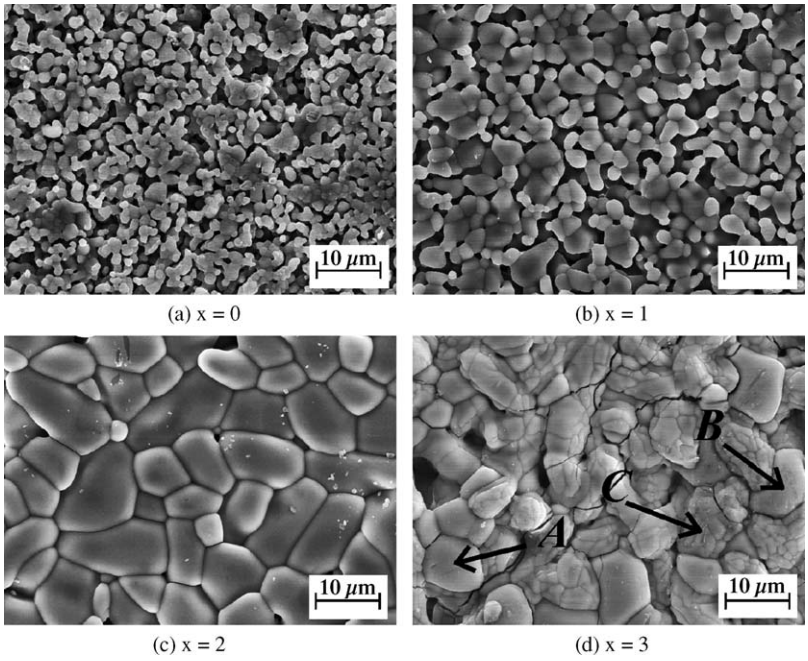

Fig. 10. Surface FE-SEM photographs of $(Mg_{3-x}Zn_x)(VO_4)_2$ ceramics sintered at 850 °C for 5 h in air where (a) $x = 0$, (b) $x = 1$, (c) $x = 2$ and (d) $x = 3$.

was observed as shown in Fig. 10(d). From the EDX analysis, the presence of $Zn_2V_2O_7$ and $Zn_4V_2O_9$ phases was observed when the sample was sintered at 850 °C. Table 2 shows the stoichiometric composition of the $Zn_2V_2O_7$ compound marked *A* and *B* in Fig. 10(d), whereas the grain marked *C* was recognized to be the stoichiometric composition of $Zn_4V_2O_9$ compound. These results are in good agreement with binary phase diagram of ZnO–V_2O_5 system.

Variation of τ_f value of the $(Mg_{3-x}Zn_x)(VO_4)_2$ sintered at various temperature is shown in Fig. 11 and then the relationship between τ_ε and τ_f values of the $(Mg_{3-x}Zn_x)(VO_4)_2$ ceramics sintered at 800 °C for 5 h in air is also shown in Fig. 12. It is generally known that the τ_f can be correlated to τ_ε by the following equation:

$$\tau_f = -\frac{1}{2}\tau_\varepsilon - \alpha \quad (1)$$

where α is the linear thermal expansion coefficient of the dielectric (α is typically in the range of 3–15 ppm/°C for most of dielectric ceramics). The τ_ε value of the sample increased with increasing x, whereas the τ_f value of the sample decreased. In the perovskite-type structure of ABO_3 compound, it is generally known that the tilting of BO_6 octahedron closely relate to the temperature dependence of dielectric constant.[9] In this study, the

Table 2
EDX data of the sample in Fig. 10(d). (wt.%)

Point	ZnO	V_2O_5
A	47.69	52.31
B	46.87	53.13
C	63.38	36.62

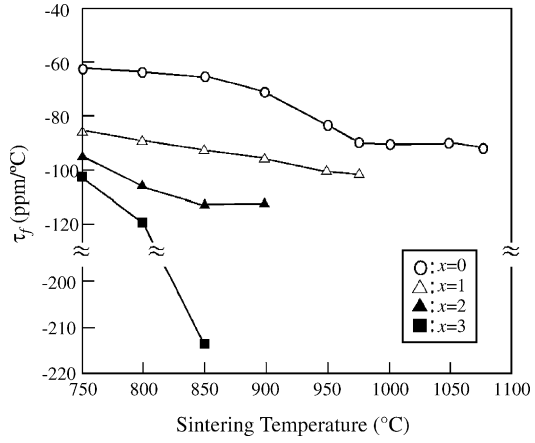

Fig. 11. Influence of sintering temperature on temperature coefficient of resonant frequency of $(Mg_{3-x}Zn_x)(VO_4)_2$ ceramics.

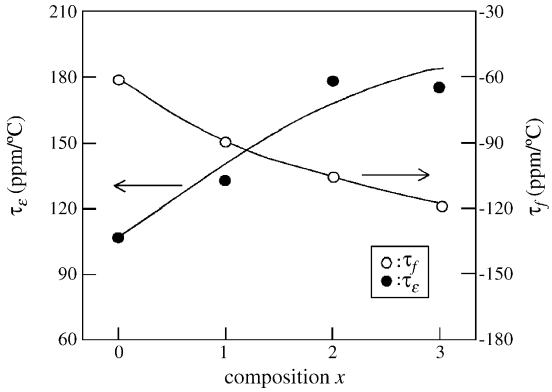

Fig. 12. Relationship between τ_ε and τ_f values of the $(Mg_{3-x}Zn_x)(VO_4)_2$ ceramics sintered at 800 °C for 5 h in air as a function of composition x.

tilting of $M(2)O_6$ is observed, as described above. Therefore, it is considered that the variations of τ_ε are caused by the tilting of $M(2)O_6$ octahedron which subsequently leads to variation in τ_f values.

4. Conclusions

The effects of Zn substitution for Mg on the microwave dielectric properties of the $(Mg_{3-x}Zn_x)(VO_4)_2$ ceramics were investigated in order to develop a new LTCC material. From the XRPD patterns, no secondary phase was detected over the whole composition range. However, the $Zn_3(VO_4)_2$ compound decomposed into $Zn_4V_2O_7$ and $Zn_2V_2O_7$ at the temperature above 850 °C. The decomposition of the $Zn_3(VO_4)_2$ compound may be related to the decrease of the microwave dielectric properties of the $(Mg_{3-x}Zn_x)(VO_4)_2$ ceramics. The decomposition was only observed over 850 °C for $x=3$. As a result, a $Q\cdot f$ value of 44709 GHz with dielectric constant of 8.1 and τ_f value of -108.2 ppm/°C was obtained for the $(Mg_{3-x}Zn_x)(VO_4)_2$ ceramics when $x=2$, sintered at the temperature of 800 °C for 5 h in air. The Zn substitution for Mg was effective in reducing the sintering temperature of the samples from 1050 to 800 °C. The normalized covalency of M–O bond decreased with increasing the composition x, and therefore, it is considered that the decrease in the covalency exerts an influence on the increase in the dielectric constant which depends on the composition x. Moreover, the τ_f value of the samples is decreased by the Zn substitution for Mg where the tilting of $M(2)O_6$ may be related to the variations in τ_f values.

References

1. Kerby, R. C. and Wilson, J. R., Solid–liquid phase equilibriums for the ternary systems vanadium (V) oxide-sodium oxide-iron (III) oxide, vanadium (V) oxide-sodium oxide-chromium (III) oxide, and vanadium (V) oxide-sodium oxide-magnesium oxide. *Can. J. Chem.*, 1973, **51**(7), 1032–1040.
2. Umemura, R., Ogawa, H., Ohsato, H. and Kan, A., Microwave dielectric properties of low-temperature sintered $Mg_3(VO_4)_2$ ceramic. *J. Eur. Ceram. Soc.*, 2005, **25**, 2865–2870.
3. Makarov, V. A., Fotiev, A. A. and Serebryakova, L. N., Phase composition and equilibrium diagram of the V_2O_5–ZnO system. *Russ. J. Inorg. Chem.*, 1971, **16**(10), 1515–1517 [Engl. Transl.].
4. Rietveld, H. M., Profile refinement method for nuclear and metal urinates. *J. Appl. Crystallogr.*, 1969, **2**, 65–71.
5. Izumi, F., In *Rietveld Method*, ed. R. A. Young. Oxford University Press, Oxford, 1993, chapter 13.
6. Hakki, B. W. and Coleman, P. D., A dielectric resonator method of measuring inductive capacities in the millimeter range. *IRE Trans: Microwave Theory & Tech.*, 1960, **MTT-8**, 402–410.
7. Brown, I. D. and Shannon, R. D., Empirical bond-strength bond-length curves for oxides. *Acta. Cryst.*, 1973, **A29**, 266.
8. Dai, S., Huang, R.-F. and Wilcox, D., Use of titanates to achieve a temperature-stable low-temperature co-fired ceramic dielectric for wireless applications. *J. Am. Ceram. Soc*, 2002, **85**(4), 828–832.
9. Thomas, N. W., Beyond the tolerance factor: harnessing X-ray and neutron diffraction data for the compositional design of perovskite ceramics. *Br. Ceram. Trans.*, 1997, **96**(1), 7–15.